Distributed Differential Modulation Over Asymmetric Fading Channels

Sara AlMaeeni, *Student Member, IEEE*, Paschalis C. Sofotasios, *Member, IEEE*, Sami Muhaidat, *Senior Member, IEEE*, George K. Karagiannidis, *Fellow, IEEE*, and Mikko Valkama, *Senior Member, IEEE*

***Abstract*—The present work quantifies the effects of asymmetric fading conditions on differentially modulated amplify-and-forward relaying systems. To this end, novel bit error rate expressions are derived for the case that the *source−relay* and *relay−destination* links experience *non-line-of-sight* multipath fading whilst the source−destination link is subject to: multipath fading, shadowing, and composite fading. Simple and tight approximate and asymptotic expressions are also derived, leading to useful insights into the system design. It is shown that the incurred performance variations range from one to few orders of magnitude compared to the standard case of symmetric Rayleigh scenarios, which verifies the importance to account for fading conditions realistically. In addition, differential phase-shift keying is shown to provide adequate performance in severe fading conditions in the moderate and high-signal-to-noise ratio regimes.**

***Index Terms*—Bit error rate (BER), differential phase-shift keying (DPSK), fading channels, relay systems.**

I. Introduction

COOPERATIVE communication is a promising emerging technology with amplify-and-forward (AF) constituting a core relaying protocol that has attracted a continuous interest over the past years. Based on this, the performance of AF systems in the context of security, generalized fading, and beamforming was analyzed in [1]–[6], respectively, whereas the typically incurred in-phase and quadrature component impairments, hardware constraints and interference effects were addressed in [7]–[9]. Likewise, the corresponding multiuser/multirelay scenarios were thoroughly addressed in [10]–[13], while useful insights on important aspects of multiantenna-based AF systems were reported in [14] and [15], and the references therein.

It is also known that multipath fading has been largely modeled by Rayleigh and Rician distributions, for the case of *non-line-of-sight* (NLOS) and *line-of-sight* (LOS) communications, respectively, whereas shadowing has been modeled by log-normal (LG), gamma, and inverse Gaussian (IG) distributions [16]–[21]. Likewise, composite distributions have been used for modeling the simultaneous occurrence of multipath fading and shadowing effects, with $K-$distribution constituting the most popular composite fading model [22]–[25].

It is known that differential phase-shift keying (DPSK) is a simple modulation technique that does not require prior channel knowledge [26]. The receiver in this case decodes the information by comparing the phase of a symbol with that of the previous symbol. To this effect, channel estimation is avoided, which leads to reduced hardware complexity. Hence, it is rendered potentially useful in the context of emerging wireless systems, which are expected to exhibit dramatically increased channel-state-information (CSI) requirements.

The performance of DPSK was analyzed extensively in [27]–[32] for different cooperative scenarios; yet, despite the usefulness of these contributions, no investigations have been reported for the case of shadowing and composite fading channels, including the important case of asymmetric fading. Motivated by this, this work quantifies the effects of asymmetric fading conditions on DPSK-based AF systems. To this end, novel analytic expressions are derived for the case of Rayleigh multipath fading in the *source-relay* (S-R) and *relay-destination* (R-D) links, and three different realistic scenarios in the *source-destination* (S-D) link, that can be encountered in practise; namely, Rician distributed multipath fading, IG distributed shadowing effects, and $K-$distributed composite fading. The offered expressions are then used in deriving simple approximate and asymptotic expressions that lead to useful insights of theoretical and practical interest. Specifically, it is shown that shadowing and composite fading effects degrade the system performance for over and nearly two orders of magnitude, respectively, than the standard Rayleigh symmetric fading case. This is exactly the opposite than in the case of LOS communications, where the corresponding performance is about two orders of magnitude better than the symmetric Rayleigh fading case. It is also shown that DPSK performs adequately at moderate and high-signal-to-noise ratio (SNR) regimes even under severe shadowing conditions.

II. System Model

We consider a half-duplex relaying system consisting of a source node S, that broadcasts a sequence of symbols, $x(n)$, to the relay terminal R and the destination terminal D. In the first time-slot, the information bits $s(n) \in \{\pm 1\}$ are differentially encoded as $x(n) = x(n-1)s(n),\ n = 1, \ldots, N$, where N is the number of bits within the frame and $x(0) = 1$. Hence, the

Manuscript received July 3, 2016; accepted August 29, 2016. Date of publication September 14, 2016; date of current version October 26, 2016. This work was supported in part by the Academy of Finland under grants 284694 and 288670. The associate editor coordinating the review of this manuscript and approving it for publication was Dr. Peter J. Schreier.

S. AlMaeeni is with the Department of Electrical and Computer Engineering, Khalifa University, Abu Dhabi 127788, UAE (e-mail: sara.a.almaeeni@ieee.org).

P. C. Sofotasios is with the Department of Electronics and Communications Engineering, Tampere University of Technology, Tampere 33101, Finland, and also with the Department of Electrical and Computer Engineering, Khalifa University, Abu Dhabi 127788, UAE (e-mail: paschalis.sofotasios@ieee.org).

S. Muhaidat is with the Department of Electrical and Computer Engineering, Khalifa University, Abu Dhabi 127788, UAE, and also with the Department of Electronic Engineering, University of Surrey, Guildford GU2 7XH, U.K. (e-mail: muhaidat@ieee.org).

G. K. Karagiannidis is with the Department of Electrical and Computer Engineering, Aristotle University of Thessaloniki, Thessaloniki 54124, Greece (e-mail: geokarag@auth.gr).

M. Valkama is with the Department of Electronics and Communications Engineering, Tampere University of Technology, Tampere 33101, Finland (e-mail: mikko.e.valkama@tut.fi).

Color versions of one or more of the figures in this letter are available online at http://ieeexplore.ieee.org.

Digital Object Identifier 10.1109/LSP.2016.2609418

received signals at the relay and destination are [27]

$$\begin{Bmatrix} y_R(n) \\ y_D(n) \end{Bmatrix} = \begin{Bmatrix} h_{S,R} \\ h_{S,D} \end{Bmatrix} x(n) + \begin{Bmatrix} w_R(n) \\ w_D(n) \end{Bmatrix} \tag{1}$$

where $h_{S,R}$ and $h_{S,D}$ denote the channel coefficients in the S-R and S-D links, respectively, and w_R and w_D denote the corresponding additive white Gaussian noise, with zero mean and variance N_0. Hence, the instantaneous SNR and average SNR for each case are expressed as $\gamma_{S,R} = |h_{S,R}|^2/N_0$, $\gamma_{S,D} = |h_{S,D}|^2/N_0$ and $\overline{\gamma}_{S,R} = \sigma^2_{S,R}/N_0$, $\overline{\gamma}_{S,D} = \sigma^2_{S,D}/N_0$, respectively, where $\sigma^2_{S,R}$ and $\sigma^2_{S,D}$ denote the respective variances. Likewise, during the second time-slot, the received signal at the relay is amplified as follows:

$$y_R^{'}(n) = \frac{y_R(n)}{\sqrt{N_0 + \sigma^2_{S,R}}} \tag{2}$$

while the signal received at the destination is represented as

$$y(n) = h_{R,D}\, y_R^{'}(n) + w_D(n) \tag{3}$$

where $h_{R,D}$ is the corresponding channel coefficient and thus, $\gamma_{R,D} = |h_{R,D}|^2/N_0$ and $\overline{\gamma}_{R,D} = \sigma^2_{R,D}/N_0$. Hence, in order to exploit the diversity from both received signals, the differential demodulation amounts to [27, eq. (7)], and the received signal is detected as in [27]–[29].

III. BER in Asymmetric Fading Conditions

A. Rayleigh S-R/R-D and Rician S-D

It is recalled that the Rician fading distribution has been used extensively in LOS scenarios. Physically, it consists of a dominant component and weaker multipath components while it includes Rayleigh fading model as a specific case [22]–[24].

Theorem 1: For $\{\overline{\gamma}_{S,R}, \overline{\gamma}_{R,D}, \overline{\gamma}_{S,D}, n\} \in \mathbb{R}^+$, the average bit error rate ($\overline{\mathrm{BER}}$) when $S-R$ and $R-D$ are Rayleigh distributed and $S-D$ is Rician distributed is given by the following closed-form expression:

$$\begin{aligned} P_{e2}^{\mathrm{Ri}} = {} & \frac{\left\{ \frac{1}{1+\overline{\gamma}_{S,D}+n^2} + \frac{\overline{\gamma}_{S,D}\left(\overline{\gamma}_{S,D}+(1+n^2)^2\right)}{4(1+\overline{\gamma}_{S,D}+n^2)^3} \right\} U(1,1,\overline{\gamma}_{R,D}^{-1})}{2\overline{\gamma}_{R,D} e^{n^2} e^{-\frac{n^2+n^4}{1+\overline{\gamma}_{S,D}+n^2}} (1+n^2)^{-1}} \\ & + \frac{\left\{ 1 + \frac{\overline{\gamma}_{S,D}\left(\overline{\gamma}_{S,D}+(1+n^2)^2\right)}{4(1+\overline{\gamma}_{S,D}+n^2)^2} \right\} (1+n^2) U(1,0,\overline{\gamma}_{R,D}^{-1})}{2(1+\overline{\gamma}_{S,R})(1+\overline{\gamma}_{S,D}+n^2) e^{-\frac{n^2+n^4}{1+\overline{\gamma}_{S,D}+n^2}+n^2}} \\ & + \frac{\left\{ \frac{U(2,1,\overline{\gamma}_{R,D}^{-1})}{2\overline{\gamma}_{R,D} e^{\frac{\overline{\gamma}_{S,D} n^2}{1+\overline{\gamma}_{S,D}+n^2}}} + \frac{e^{-n^2} U(2,0,\overline{\gamma}_{R,D}^{-1})}{(1+\overline{\gamma}_{S,R}) e^{-\frac{n^2+n^4}{1+\overline{\gamma}_{S,D}+n^2}}} \right\}}{4\overline{\gamma}_{S,R}^{-1}(1+\overline{\gamma}_{S,R})(1+\overline{\gamma}_{S,D}+n^2)(1+n^2)^{-1}} \end{aligned} \tag{4}$$

where $U(\cdot,\cdot,\cdot)$ is the confluent hypergeometric function of the second kind [33] and $n \geq 0$ is the Nakagami$-n$ parameter which is related to the Rician K factor by $K = n^2$ [22].

Proof: The end-to-end BER is given by [27, eq. (14)], namely

$$P_{e2} = \int_0^\infty \int_0^\infty \frac{4+\gamma_{\mathrm{eq}}+\gamma_{S,D}}{8} \frac{p(\gamma_{\mathrm{eq}})p(\gamma_{S,D})}{e^{\gamma_{\mathrm{eq}}+\gamma_{S,D}}} \mathrm{d}\gamma_{\mathrm{eq}} \mathrm{d}\gamma_{S,D}. \tag{5}$$

For the case of Rayleigh distributed S-R and R-D paths, the PDF of γ_{eq} is represented by [27, eq. (9)]. In the same context, when the S-D is Rician distributed, it follows that:

$$p(\gamma_{S,D}) = \frac{(1+n^2)e^{-n^2}}{\overline{\gamma}_{S,D} e^{\frac{(1+n^2)\gamma_{S,D}}{\overline{\gamma}_{S,D}}}} I_0\left(2n\sqrt{\frac{(1+n^2)\gamma_{S,D}}{\overline{\gamma}_{S,D}}}\right) \tag{6}$$

where I_0 is the modified Bessel function of the first kind [33]. Thus, substituting [27, eq. (9)] and (6) in (5) yields (7) as shown at the bottom of this page, where

$$\begin{Bmatrix} \mathcal{I}_1 \\ \mathcal{I}_2 \end{Bmatrix} = \int_0^\infty \begin{Bmatrix} 1 \\ \gamma_{S,D} \end{Bmatrix} \frac{I_0\left(2n\sqrt{\frac{(1+n^2)\gamma_{S,D}}{\overline{\gamma}_{S,D}}}\right)}{e^{\gamma_{S,D}+\frac{(1+n^2)\gamma_{S,D}}{\overline{\gamma}_{S,D}}}} \mathrm{d}\gamma_{S,D} \tag{8}$$

and $\beta = 2\sqrt{(1+\overline{\gamma}_{sr})}/\sqrt{\overline{\gamma}_{sr}\overline{\gamma}_{rd}}$ while $K_n(x)$ denotes the modified Bessel function of the second kind. Importantly, the above two integrals can be expressed in closed-form using [33, eq. (6.643.2)] and [33, eq. (6.643.3)], respectively, with a, c, μ and ν parameters denoting arbitrary reals. Thus, making the necessary variable transformation and substituting into (7) yields (4), which completes the proof. ■

It is noted that (4) can be readily computed since the involved functions are built-in in popular software packages such as MAPLE, MATHEMATICA, and MATLAB. Furthermore, for $\overline{\gamma}_{R,D} >> 0$, it follows that $U(1,0,\overline{\gamma}_{R,D}^{-1} \to 0) \to 1$ and $U(2,0,\overline{\gamma}_{R,D}^{-1} \to 0) \to 1/2$, whereas $U(1,1,\overline{\gamma}_{R,D}^{-1})$ and $U(2,1,\overline{\gamma}_{R,D}^{-1})$ can be expressed in terms of the lower incomplete gamma function, $\Gamma(0,x)$, [33]. Based on this, one obtains

$$P_{e2}^{\mathrm{Ri}} \simeq \frac{5(1+n^2)e^{-n^2}}{8\overline{\gamma}_{S,D}\overline{\gamma}_{R,D}} \left\{ 1 + \Gamma\left(0, \frac{1}{\overline{\gamma}_{R,D}}\right) \right\} \tag{9}$$

which for $\overline{\gamma}_{R,D} >> 0$, it reduces to a simple asymptotic expression that involves only elementary functions, namely

$$P_{e2}^{\mathrm{Ri}} \longrightarrow \frac{6(1+n^2)e^{-n^2}}{\overline{\gamma}_{S,D}\overline{\gamma}_{R,D}} \tag{10}$$

which are also readily computed and provide insights on the effect of the involved parameters on the system performance.

$$\begin{aligned} P_{e2}^{\mathrm{Ri}} = {} & \frac{\mathcal{I}_1\,(1+n^2)(1+\overline{\gamma}_{S,R})}{\overline{\gamma}_{S,D}\overline{\gamma}_{S,R}\overline{\gamma}_{R,D}e^{n^2}} \int_0^\infty \frac{e^{-\frac{\gamma_{\mathrm{eq}}}{\overline{\gamma}_{S,R}}}}{e^{\gamma_{\mathrm{eq}}}} K_0(\beta\sqrt{\gamma_{\mathrm{eq}}}) \mathrm{d}\gamma_{\mathrm{eq}} + \frac{\mathcal{I}_1\,(1+n^2)\sqrt{1+\overline{\gamma}_{S,R}}}{\overline{\gamma}_{S,D}\overline{\gamma}_{S,R}\sqrt{\overline{\gamma}_{S,R}\overline{\gamma}_{R,D}}e^{n^2}} \int_0^\infty \frac{\sqrt{\gamma_{\mathrm{eq}}}\, K_1(\beta\sqrt{\gamma_{\mathrm{eq}}})}{e^{\gamma_{\mathrm{eq}}+\frac{\gamma_{\mathrm{eq}}}{\overline{\gamma}_{S,R}}}} \mathrm{d}\gamma_{\mathrm{eq}} \\ & + \frac{\mathcal{I}_1\,(1+n^2)(1+\overline{\gamma}_{S,R})}{4\overline{\gamma}_{S,D}\overline{\gamma}_{S,R}\overline{\gamma}_{R,D}e^{n^2}} \int_0^\infty \frac{\gamma_{\mathrm{eq}}\, K_0(\beta\sqrt{\gamma_{\mathrm{eq}}})}{e^{\gamma_{\mathrm{eq}}+\frac{\gamma_{\mathrm{eq}}}{4\overline{\gamma}_{S,R}}}} \mathrm{d}\gamma_{\mathrm{eq}} + \frac{\mathcal{I}_1\,(1+n^2)\sqrt{1+\overline{\gamma}_{S,R}}}{4\overline{\gamma}_{S,D}\overline{\gamma}_{S,R}\sqrt{\overline{\gamma}_{S,R}\overline{\gamma}_{R,D}}e^{n^2}} \int_0^\infty \frac{\gamma_{\mathrm{eq}}^{3/2}\, K_1(\beta\sqrt{\gamma_{\mathrm{eq}}})}{e^{\gamma_{\mathrm{eq}}+\frac{\gamma_{\mathrm{eq}}}{4\overline{\gamma}_{S,R}}}} \mathrm{d}\gamma_{\mathrm{eq}} \\ & + \frac{\mathcal{I}_2\,(1+n^2)(1+\overline{\gamma}_{S,R})}{4\overline{\gamma}_{S,D}\overline{\gamma}_{S,R}\overline{\gamma}_{R,D}e^{n^2}} \int_0^\infty \frac{e^{-\frac{\gamma_{\mathrm{eq}}}{4\overline{\gamma}_{S,R}}}}{e^{\gamma_{\mathrm{eq}}}} K_0(\beta\sqrt{\gamma_{\mathrm{eq}}}) \mathrm{d}\gamma_{\mathrm{eq}} + \frac{\mathcal{I}_2\,(1+n^2)\sqrt{1+\overline{\gamma}_{S,R}}}{4\overline{\gamma}_{S,D}\overline{\gamma}_{S,R}\sqrt{\overline{\gamma}_{S,R}\overline{\gamma}_{R,D}}e^{n^2}} \int_0^\infty \frac{\sqrt{\gamma_{\mathrm{eq}}}\, K_1(\beta\sqrt{\gamma_{\mathrm{eq}}})}{e^{\gamma_{\mathrm{eq}}+\frac{\gamma_{\mathrm{eq}}}{4\overline{\gamma}_{S,R}}}} \mathrm{d}\gamma_{\mathrm{eq}} \end{aligned} \tag{7}$$

B. Rayleigh S-R/R-D and IG S-D

LG distribution has been considered accurate in modeling large-scale fading effects. However, its relatively intractable representation has led to the proposition of the IG model, which has been shown to be the most accurate substitute to LG for modeling shadowing [16]–[21].

Theorem 2: For $\{\overline{\gamma}_{S,R}, \overline{\gamma}_{R,D}, \overline{\gamma}_{S,D}\} \in \mathbb{R}^+$ and shape parameter $\lambda \in \mathbb{R}$, the following closed-form expression holds for the $\overline{\mathrm{BER}}$, when the S-R and R-D links are Rayleigh distributed and the S-D link is inversely Gaussian distributed

$$P_{e2}^{\mathrm{IG}} = \frac{\overline{\gamma}_{S,R} e^{-\sqrt{\lambda}\sqrt{2+\frac{\lambda}{\overline{\gamma}^2_{S,D}}}}}{4(1+\overline{\gamma}_{S,R}) e^{-\frac{\lambda}{\overline{\gamma}_{S,D}}}} \left\{ \frac{U(2,0,\overline{\gamma}^{-1}_{R,D})}{(1+\overline{\gamma}_{S,R})} + \frac{U(2,1,\overline{\gamma}^{-1}_{R,D})}{2\overline{\gamma}_{R,D}} \right\} + \frac{e^{\frac{\lambda}{\overline{\gamma}_{S,D}}} U(1,0,\overline{\gamma}^{-1}_{R,D})}{2\,(1+\overline{\gamma}_{S,R}) e^{\sqrt{\lambda}\sqrt{2+\frac{\lambda}{\overline{\gamma}^2_{S,D}}}}} \left\{ 1 + \frac{\sqrt{\lambda}}{4\sqrt{2+\frac{\lambda}{\overline{\gamma}^2_{S,D}}}} \right\} + \frac{e^{\frac{\lambda}{\overline{\gamma}_{S,D}}}\, U(1,1,\overline{\gamma}^{-1}_{R,D})}{2\overline{\gamma}_{R,D}\, e^{\sqrt{\lambda}\sqrt{2+\frac{\lambda}{\overline{\gamma}^2_{S,D}}}}} \left\{ 1 + \frac{\sqrt{\lambda}}{4\sqrt{2+\frac{\lambda}{\overline{\gamma}^2_{S,D}}}} \right\}. \quad (11)$$

Proof: The $p(\gamma_{\mathrm{eq}})$ when S-R and R-D links are Rayleigh distributed is given by [27, eq. (9)]. Likewise, when the S-D path experiences IG shadowing effects it follows that [17], [18]:

$$p(\gamma_{S,D}) = \sqrt{\frac{\lambda}{2\pi\gamma^3_{S,D}}} e^{-\frac{\lambda(\gamma_{S,D}-\overline{\gamma}_{S,D})^2}{2\gamma_{S,D}\overline{\gamma}^2_{S,D}}}. \quad (12)$$

Hence, by substituting [27, eq. (9)] and (12) into (5) yields

$$P_{e2}^{\mathrm{IG}} = \frac{(4\mathcal{I}_3+\mathcal{I}_4)\sqrt{1+\overline{\gamma}_{S,R}}}{4\overline{\gamma}_{S,R}\sqrt{\overline{\gamma}_{S,R}\overline{\gamma}_{R,D}}} \int_0^\infty \frac{\sqrt{\gamma_{\mathrm{eq}}} K_1(\beta\sqrt{\gamma_{\mathrm{eq}}})}{e^{\gamma_{\mathrm{eq}}\left(1+\frac{1}{\overline{\gamma}_{S,R}}\right)}} \mathrm{d}\gamma_{\mathrm{eq}} + \frac{\mathcal{I}_4\sqrt{1+\overline{\gamma}_{S,R}}}{4\overline{\gamma}_{S,R}\sqrt{\overline{\gamma}_{S,R}\overline{\gamma}_{R,D}}} \int_0^\infty \frac{\sqrt{\gamma_{\mathrm{eq}}} K_1(\beta\sqrt{\gamma_{\mathrm{eq}}})}{e^{\gamma_{\mathrm{eq}}\left(1+\frac{1}{\overline{\gamma}_{S,R}}\right)}} \mathrm{d}\gamma_{\mathrm{eq}} + \frac{(4\mathcal{I}_3+\mathcal{I}_4)(\overline{\gamma}_{S,R}+1)}{4\overline{\gamma}_{S,R}\overline{\gamma}_{R,D}} \int_0^\infty \frac{K_0(\beta\sqrt{\gamma_{\mathrm{eq}}})}{e^{\gamma_{\mathrm{eq}}\left(1+\frac{1}{\overline{\gamma}_{S,R}}\right)}} \mathrm{d}\gamma_{\mathrm{eq}} + \frac{\mathcal{I}_3(\overline{\gamma}_{S,R}+1)}{4\overline{\gamma}_{S,R}\overline{\gamma}_{R,D}} \int_0^\infty \frac{\gamma_{\mathrm{eq}} K_0(\beta\sqrt{\gamma_{\mathrm{eq}}})}{e^{\gamma_{\mathrm{eq}}\left(1+\frac{1}{\overline{\gamma}_{S,R}}\right)}} \mathrm{d}\gamma_{\mathrm{eq}} \quad (13)$$

where

$$\left\{ \begin{matrix} \mathcal{I}_3 \\ \mathcal{I}_4 \end{matrix} \right\} = \int_0^\infty \left\{ \begin{matrix} \gamma^{-1}_{S,D} \\ 1 \end{matrix} \right\} \frac{e^{-\gamma_{S,D}\left(1+\frac{\lambda}{2\overline{\gamma}^2_{S,D}}\right)} e^{-\frac{\lambda}{2\gamma_{S,D}}}}{\sqrt{\gamma_{S,D}} e^{-\frac{\lambda}{\overline{\gamma}_{S,D}}}} \mathrm{d}\gamma_{S,D}. \quad (14)$$

The integrals in (13) constitute special cases of the generic integral $\int_0^\infty x^\mu \exp(-\mathrm{a}\,\mathrm{x}) K_\nu(c\sqrt{x})\mathrm{d}x$, which can be expressed in closed-form using [33, eq. (6.643.3)]. Likewise, the $\mathcal{I}_3$ and $\mathcal{I}_4$ integrals are special cases of the generic integral $\int_0^\infty x^\mu \exp(-\mathrm{a}\,\mathrm{x} - b/x)\mathrm{d}x$, which can be expressed in closed-form according to [33, eq. (3.471.9)]. To this effect, by performing a necessary change of variables in (14) and substituting in (13) yields (11), which completes the proof. ■

Evidently, the derived exact closed-form solution in (11) involves the same hypergeometric functions as in (4) of Theorem 1. To this effect and using their aforementioned properties along with lengthy but basic algebraic manipulations yields

$$P_{e2}^{\mathrm{IG}} \simeq \frac{\overline{\gamma}_{S,R}\Gamma\left(0,\overline{\gamma}^{-1}_{R,D}\right) + 2\overline{\gamma}_{R,D}}{2\overline{\gamma}_{R,D}\overline{\gamma}_{S,R} e^{\sqrt{2\lambda}}\left(1+\frac{\sqrt{\lambda}}{2^{5/2}}\right)^{-1}} + \frac{\Gamma(0,\overline{\gamma}^{-1}_{R,D})}{8\,\overline{\gamma}^2_{R,D}\, e^{\sqrt{2\lambda}}} \quad (15)$$

and

$$P_{e2}^{\mathrm{IG}} \longrightarrow \frac{(5\overline{\gamma}_{S,R}+\overline{\gamma}_{R,D}) e^{-\sqrt{2\lambda}}}{\overline{\gamma}_{R,D}\overline{\gamma}_{S,R}\left(1+\frac{\sqrt{\lambda}}{2^{5/2}}\right)^{-1}} + \frac{5e^{-\sqrt{2\lambda}}}{4\,\overline{\gamma}^2_{R,D}} \quad (16)$$

which exhibit the effects of the average SNRs and the shadowing parameter λ at both moderate- and high-SNR regimes, while they have a simple and straightforwardly computed form.

C. Rayleigh S-R/R-D and K−Distributed S-D

It is recalled that Rayleigh/gamma or $K-$distribution has been used extensively in accounting for the simultaneous occurrence of multipath and shadowing, which is a realistic communication scenario that is encountered often in practice.

Theorem 3: For $\{\overline{\gamma}_{S,R}, \overline{\gamma}_{R,D}, \overline{\gamma}_{S,D}, k\} \in \mathbb{R}^+$, the following expression holds for the $\overline{\mathrm{BER}}$ when S-R and R-D links are Rayleigh distributed and S-D link is K−distributed:

$$P_{e2}^{\mathrm{K}} = \frac{U(1+k,k,k\overline{\gamma}^{-1}_{S,D})}{8\,k^{-k-1}\,\overline{\gamma}^k_{S,D}} \left\{ \frac{U(1,1,\overline{\gamma}^{-1}_{R,D})}{\overline{\gamma}_{R,D}} + \frac{U(1,0,\overline{\gamma}^{-1}_{R,D})}{1+\overline{\gamma}_{S,R}} \right\} + \frac{k^k\, U(k,k,k\overline{\gamma}^{-1}_{S,D})}{2\overline{\gamma}^k_{S,D}} \left\{ \frac{U(1,1,\overline{\gamma}^{-1}_{R,D})}{\overline{\gamma}_{R,D}} + \frac{U(1,0,\overline{\gamma}^{-1}_{R,D})}{1+\overline{\gamma}_{S,R}} + \frac{\overline{\gamma}_{S,R}\, U(2,1,\overline{\gamma}^{-1}_{R,D})}{4\overline{\gamma}_{R,D}(1+\overline{\gamma}_{S,R})} + \frac{\sqrt{1+\overline{\gamma}_{S,R}} U(2,0,\overline{\gamma}^{-1}_{R,D})}{2(1+\overline{\gamma}_{S,R})^{5/2}\,\overline{\gamma}^{-1}_{S,R}} \right\} \quad (17)$$

where k denotes the shape parameter of the distribution.

Proof: When the direct link experiences composite fading effects that follow the $K-$distribution, one obtains [22]:

$$p(\gamma_{S,D}) = \frac{2k^{\frac{k+1}{2}}}{\overline{\gamma}^{\frac{k+1}{2}}_{S,D}\Gamma(k)} \gamma^{\frac{k-1}{2}}_{S,D} K_{k-1}\left(2\sqrt{\frac{k\gamma_{S,D}}{\overline{\gamma}_{S,D}}}\right). \quad (18)$$

By substituting (18) and [27, eq. (9)] into (5), and carrying out long but basic algebraic manipulations it follows that:

$$P_{e2}^{\mathrm{K}} = \frac{(4\mathcal{I}_5+\mathcal{I}_6)\sqrt{1+\overline{\gamma}_{S,R}}}{4\overline{\gamma}_{S,R}\sqrt{\overline{\gamma}_{S,R}\overline{\gamma}_{R,D}}} \int_0^\infty \frac{\sqrt{\gamma_{\mathrm{eq}}} K_1(\beta\sqrt{\gamma_{\mathrm{eq}}})}{e^{\gamma_{\mathrm{eq}}\left(1+\frac{1}{\overline{\gamma}_{S,R}}\right)}} \mathrm{d}\gamma_{\mathrm{eq}} + \frac{\mathcal{I}_5\sqrt{1+\overline{\gamma}_{S,R}}}{4\overline{\gamma}_{S,R}\sqrt{\overline{\gamma}_{S,R}\overline{\gamma}_{R,D}}} \int_0^\infty \frac{\gamma_{\mathrm{eq}}\sqrt{\gamma_{\mathrm{eq}}} K_1(\beta\sqrt{\gamma_{\mathrm{eq}}})}{e^{\gamma_{\mathrm{eq}}\left(1+\frac{1}{\overline{\gamma}_{S,R}}\right)}} \mathrm{d}\gamma_{\mathrm{eq}} + \frac{(4\mathcal{I}_5+\mathcal{I}_6)(\overline{\gamma}_{S,R}+1)}{4\overline{\gamma}_{S,R}\overline{\gamma}_{R,D}} \int_0^\infty \frac{K_0(\beta\sqrt{\gamma_{\mathrm{eq}}})}{e^{\gamma_{\mathrm{eq}}\left(1+\frac{1}{\overline{\gamma}_{S,R}}\right)}} \mathrm{d}\gamma_{\mathrm{eq}} + \frac{\mathcal{I}_5(\overline{\gamma}_{S,R}+1)}{4\overline{\gamma}_{S,R}\overline{\gamma}_{R,D}} \int_0^\infty \frac{\gamma_{\mathrm{eq}} K_0(\beta\sqrt{\gamma_{\mathrm{eq}}})}{e^{\gamma_{\mathrm{eq}}\left(1+\frac{1}{\overline{\gamma}_{S,R}}\right)}} \mathrm{d}\gamma_{\mathrm{eq}} \quad (19)$$

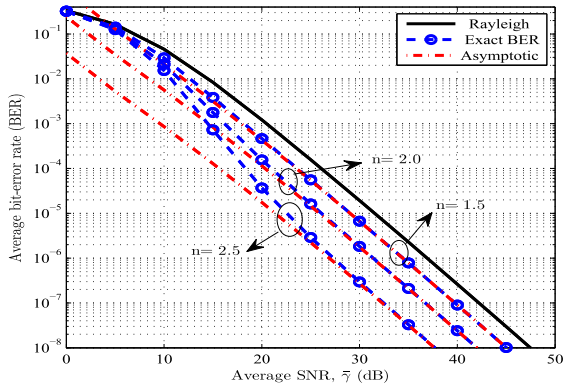

Fig. 1. $\overline{\mathrm{BER}}$ versus $\overline{\gamma}$ for DPSK in Rayleigh S-R/R-D and Rice S-D.

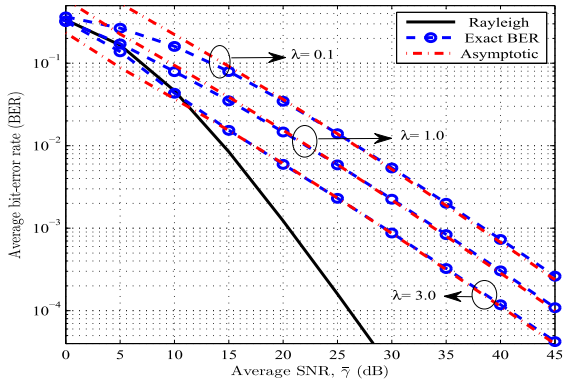

Fig. 2. $\overline{\mathrm{BER}}$ versus $\overline{\gamma}$ for DPSK in Rayleigh S-R/R-D and IG S-D.

where

$$\left\{\begin{matrix}\mathcal{I}_5\\ \mathcal{I}_6\end{matrix}\right\} = \frac{2k^{\frac{k+1}{2}}}{\overline{\gamma}_{S,D}^{\frac{k+1}{2}}\Gamma(k)}\int_0^\infty \frac{\gamma_{S,D}^{\frac{k\{\mp\}1}{2}}}{e^{\gamma_{S,D}}} K_{k-1}\left(2\sqrt{\frac{k\gamma_{S,D}}{\overline{\gamma}_{S,D}}}\right)\mathrm{d}\gamma_{S,D}. \tag{20}$$

The integrals in (19) have the same form as (7) and (13), as well as the integrals $\mathcal{I}_5$ and $\mathcal{I}_6$. Thus, by making the necessary change of variables in [33, eq. (6.643.3)] and substituting in (20) and (19) yields (17), which completes the proof. ■

IV. Numerical Results

This section utilizes the offered results to quantify the effects of asymmetric fading conditions on the considered scenarios. To this end, binary DPSK, equal power allocation, and symmetric values for average SNRs are assumed indicatively in all cases, i.e., $\overline{\gamma}_{S,D} = \overline{\gamma}_{S,R} = \overline{\gamma}_{R,D} = \overline{\gamma}$. Fig. 1 illustrates the $\overline{\mathrm{BER}}$ versus $\overline{\gamma}$ and different values of n for scenario 1, which is practically encountered in uplink/downlink scenarios that involve LOS components in the direct link. As expected, the value of n affects significantly the system performance since, indicatively, $\overline{\mathrm{BER}}$ improves by a difference of almost three orders of magnitude between $n = 1.5$ and $n = 4$ at $\overline{\gamma} = 17.5$ dB. This behavior is also noticed when comparing to the case that the direct path is Rayleigh distributed, that verifies the significance of a dominant component across all SNR regimes. In addition, it is shown that the derived asymptotic expression is accurate even for moderate values of $\overline{\gamma}$, as it is rather tight at moderate- and high-SNR regimes.

On the contrary, when the direct link is IG distributed, the overall performance reduces dramatically over the whole range of SNR values. This indicates the significantly detrimental effects of shadowing, as the average BER for severe conditions is around 10^{-1} for $\overline{\gamma} = 15$ dB and worse than 10^{-4} for $\overline{\gamma} = 45$ dB. It is also demonstrated that the effects of shadowing are substantially more severe than those of multipath, particularly in the high-SNR regime. In fact, by recalling that Rayleigh fading corresponds to severe multipath fading conditions, compared to, e.g., Nakagami-4 conditions, it becomes evident that shadowing effects dominate clearly those of multipath fading as a difference of nearly two orders of magnitude is observed in Fig. 2 between shadowed and multipath scenarios at moderate values of $\overline{\gamma}$. Given also that this type of scenarios are encountered in long-distance communications, where fundamentally shadowing prevails, it is crucial to account for shadowing effects realistically. This tends to be the case also in composite fading conditions as the corresponding performance degradation is substantially higher than the one owed to multipath fading and

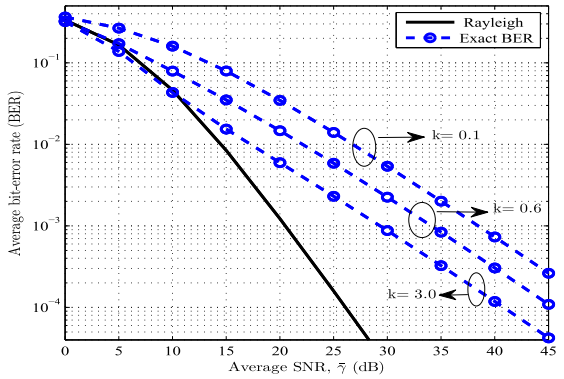

Fig. 3. $\overline{\mathrm{BER}}$ versus $\overline{\gamma}$ for DPSK in Rayleigh S-R/R-D and K S-D.

it practically approaches the severity of shadowing conditions, particularly in the high-SNR regime. This is illustrated in Fig. 3, where it is indicatively observed that the $\overline{\mathrm{BER}}$ for severe fading conditions is around 10^{-2} at $\overline{\gamma} = 25$ dB and slightly better than 10^{-3} at $\overline{\gamma} = 40$ dB. Hence, the effects of composite fading should also not be neglected in the design of emerging wireless communications systems, which often consider only multipath effects, as this can result to inaccurate performance expectations and in turn to problematic system deployments.

Finally, the considered scenarios demonstrate that differential modulation provides an adequate performance in all multipath fading conditions as well as under severe shadowing and composite fading, at moderate- and high-SNR regimes. This shows that it can be considered a suitable option for low complexity systems and particularly in cases with increased CSI requirements. Therefore, it can be a complementary useful solution in emerging wireless communications, since future deployments are expected to exhibit undesirably long overheads and substantially increased system complexities.

V. Conclusion

This work quantified the effects of multipath fading, shadowing, and composite fading in AF relay systems over asymmetric fading channels, which are practically encountered in realistic uplink/downlink communications in the context of LOS/NLOS and short/long distance transmissions. It was shown that these effects have a detrimental impact on the system performance and that shadowing dominates significantly in the high-SNR regime. Furthermore, it was shown that DPSK provides adequate performance in both low- and high-SNR regimes even in severe fading conditions. This renders it a suitable modulation scheme for reduced complexity deployments.

REFERENCES

[1] Y. Liu, L. Wang, T. T. Duy, M. Elkashlan, and T. Q. Duong, "Relay selection for security enhancement in cognitive relay networks," *IEEE Wireless Commun. Lett.*, vol. 4, no. 1, pp. 46–49, Jan. 2015.

[2] J. Yang, L. Chen, X. Lei, K. P. Peppas, and T. Q. Duong, "Dual-hop cognitive amplify-and-forward relaying networks over $\eta - \mu$ fading channels," *IEEE Trans. Veh. Technol.*, vol. 65, no. 8, pp. 6290–6300, Aug. 2015.

[3] W. Xu, J. Zhang, Y. Liu, and P. Zhang, "Performance analysis of semi-blind amplify-and-forward relay system in mixed Nakagami-*m* and Rician fading channels," *IEICE Trans. Commun.*, vol. E93-B, no. 11, pp. 3137–3140, Nov. 2010

[4] K. P. Peppas, G. C. Alexandropoulos, and P. T. Mathiopoulos, "Performance analysis of dual-hop AF relaying systems over mixed and fading channels," *IEEE Trans. Veh. Technol.*, vol. 62, no. 7, pp. 3149–3163, Sep. 2013.

[5] H. Ding, J. Ge, D. B. da Costa, and Y. Guo, "Outage analysis for multiuser two-way relaying in mixed Rayleigh and Rician fading," *IEEE Commun. Lett.*, vol. 15, no. 4, pp. 410–412, Apr. 2011.

[6] H. A. Suraweera, T. A Tsiftsis, G. K Karagiannidis, and A. Nallanathan, "Effect of feedback delay on amplify-and-forward relay networks with beamforming," *IEEE Trans. Veh. Technol.*, vol. 60, no. 3, pp. 1265–1271, Mar. 2011.

[7] J. Li, M. Matthaiou, and T. Svensson, "I/Q imbalance in AF dual-hop relaying: Performance analysis in Nakagami-m fading," *IEEE Trans. Commun.*, vol. 62, no. 3, pp. 836–847, Mar. 2014.

[8] G. Zhu, C. Zhong, H. A. Suraweera, Z. Zhang, C. Yuen and R. Yin, "Ergodic capacity comparison of different relay precoding schemes in dual-hop AF systems with co-channel interference," *IEEE Trans. Commun.*, vol. 62, no. 7, pp. 2314–2328, Jul. 2014.

[9] T. T. Duy, T. Q. Duong, D. B. da Costa, V. N. Q. Bao, and M. Elkashlan, "Proactive relay selection with joint impact of hardware impairment and co-channel interference," *IEEE Trans. Commun.*, vol. 63, no. 5, pp. 1594–1606, May 2015.

[10] J. Yang, P. Fan, T. Q. Duong and X. Lei, "Exact performance of two-way relay networks in Nakagami-m fading," *IEEE Trans. Wireless Commun.*, vol. 10, no. 3, pp. 980–987, Mar. 2011.

[11] L. Fan, X. Lei, T. Q. Duong, R. Q. Hu, and M. Elkashlan, "Multiuser cognitive relay networks: Joint impact of direct and relay communications," *IEEE Trans. Wireless Commun.*, vol. 13, no. 9, pp. 5043–5055, Sep. 2014.

[12] Y. Lu, N. Yang, M. Elkashlan, and J. Yuan, "Partial channel quality information feedback in multiuser relay networks over Nakagami$-m$ fading," *IEEE Trans. Wireless Commun.*, vol. 14, no. 9, pp. 4783–4796, Sep. 2015.

[13] J. Xu, T. Ratnarajah, M. Sellathurai, and Z. Ding, "Performance analysis for multi-way relaying in Rician fading channels," *IEEE Trans. Commun.*, vol. 63, no. 11, pp. 4050–4062, Nov. 2015.

[14] E. Soleimani-Nasab, M. Matthaiou, and M. Ardebilipour, "Multi-relay MIMO systems with OSTBC over Nakagami$-m$ fading channels," *IEEE Trans. Veh. Technol.* vol. 62, no. 8, pp. 3721–3736, Oct. 2013.

[15] G. Zhu, C. Zhong, H. A. Suraweera, Z. Zhang and C. Yuen, "Outage probability of dual-hop multiple antenna AF systems with linear processing in the presence of co-channel interference," *IEEE Trans. Wireless Commun.*, vol. 13, no. 4, pp. 2308–2321, Apr. 2014.

[16] Karmeshu and R. Agrawal, "On efficacy of Rayleigh-inverse Gaussian distribution over $K-$distribution for wireless fading channels," *Wireless Commun. Mobile Comput.*, vol. 7, no. 1, pp. 1–7, Jan. 2007.

[17] N. D. Chatzidiamantis, H. G. Sandalidis, G. K. Karagiannidis, and S. Kotsopoulos, "On the inverse-Gaussian shadowing," in *Proc. 2011 IEEE Int. Conf. Commun. Inf. Technol.*, Mar. 2011, pp. 142–146.

[18] I. Trigui, A. Laourine, S. Affes, and A. Stephenne, "The inverse Gaussian distribution in wireless channels: second-order statistics and channel capacity," *IEEE Trans. Commun.*, vol. 60, no. 11, pp. 3167–3173, Nov. 2012.

[19] P. C. Sofotasios, T. A. Tsiftsis, M. Ghogho, L. R. Wilhelmsson, and M. Valkama, "The $\eta - \mu$/inverse-Gaussian distribution: A novel physical multipath /shadowing F fading model," *IEEE Int. Conf. Commun., Budapest, Hungary*, Jun. 2013, pp. 5715–5719.

[20] C. Zhong, M. Matthaiou, G. K. Karagiannidis, A. Huang, and Z. Zhang, "Capacity bounds for AF dual-hop relaying in G fading channels," *IEEE Trans. Veh. Technol.*, vol. 61, no. 4, pp. 1730–1740, May 2012.

[21] P. C. Sofotasios, T. A. Tsiftsis, K. Ho-Van, S. Freear, L. R. Wilhelmsson, and M. Valkama, "The $\kappa - \mu$/Inverse-Gaussian composite statistical distribution in RF and FSO wireless channels," in *Proc. 2013 IEEE 78th Veh. Technol. Conf*, Las Vegas, NV, USA, Sep. 2013, pp. 1–5.

[22] M. K. Simon and M.-S. Alouni, *Digital Communication Over Fading Channels*, 2nd ed. New York, NY, USA: Wiley, 2005.

[23] D. A Zogas and G. K Karagiannidis, "Infinite-series representations associated with the bivariate Rician distribution and their applications," *IEEE Trans. Commun.*, vol. 53, no. 11, pp. 1790–1794, Nov. 2005.

[24] P. C. Sofotasios and S. Freear, "Novel expressions for the one and two dimensional Gaussian $Q-$functions," in *Proc. 2010 IEEE Int. Conf. Wireless Inf. Technol. Syst.*, Honolulu, HI, USA, 2010, pp. 1–4.

[25] J. F. Paris, P. C. Sofotasios, and T. A. Tsiftsis, "Special issue on advances in statistical channel modeling for wireless communications," *Hindawi Int. J. Ant. Propag.*, vol. 2015, 2015, Art. no. 541619.

[26] S. Muhaidat, P. Ho, and M. Uysal, "Distributed differential space-time coding for broadband cooperative networks," in *Proc. IEEE 69th Veh. Technol. Conf.*, Barcelona, Spain, Apr. 2009, pp. 1–6.

[27] Q. Zhao and H. Li, "Performance of differential modulation with wireless relays in Rayleigh fading channels," *IEEE Commun. Lett*. vol. 9, no. 4, pp. 343–345, Apr. 2005.

[28] T. Cui, F. Gao, and C. Tellambura, "Differential modulation for cooperative wireless systems," *IEEE Trans. Commun.*, vol. 57, no. 10, pp. 2977–2987, Oct. 2009.

[29] Q. Zhao and H. Li, "Performance analysis of an amplify-based differential modulation for wireless relay networks under Nakagami$-m$ fading channels," in *Proc. 2005 IEEE 6th Workshop Signal Process. Adv. Wireless Commun.*, Jun. 2005, pp. 211–215.

[30] M. R. Bhatnagar, "DF-based differential modulation for cooperative communication system with unitary and nonunitary constellations," *IEEE Trans. Veh. Technol.*, vol. 61, no. 1, pp. 152–165, Jan. 2012.

[31] Q. Zhao and H. Li, "Differential modulation for cooperative wireless systems," *IEEE Trans. Signal Process.*, vol. 55, no. 5, pp. 2273–2283, Oct. 2007.

[32] M. R. Bhatnagar, "Average BER analysis of differential modulation in DF cooperative communication system over Gamma–Gamma fading FSO links," *IEEE Commun, Lett.* vol. 16, no. 8, pp. 1228–1231, Aug. 2012.

[33] I. S. Gradshteyn and I. M. Ryzhik, *Table of Integrals, Series, and Products*, 7th ed., New York, NY, USA: Academic, 2007.